



SG-8

## DEFORMATION BEHAVIOR OF SHEAR WALLS AFTER FLEXURAL YIELDING

Hisahiro HIRAIISHI<sup>1</sup> and Toshikazu KAWASHIMA<sup>2</sup>

<sup>1</sup>Head, Structure Division, Building Research Institute, Ministry of  
Construction, Tukuba-shi, Ibaraki, Japan

<sup>2</sup>Research Assistant, Structure Division, Building Research Institute,  
Ministry of Construction, Tukuba-shi, Ibaraki, Japan

### SUMMARY

Test data of multistory shear walls under lateral static loads indicated that a stable region of deformation where the deformation profile along the height did not change followed after flexural yielding. In this stable region, the drift angle of each story was equal to the drift angle and to the rotation just above the hinging region. The drift of the upper stories increased very little after the limit of this stable region even though the drift of the first story increased significantly. The deformation of the shear walls was estimated excellently by the truss model which consists of a single non-prismatic member and rigid members, and rotates around the base of the boundary column under compression.

### INTRODUCTION

The deformation behavior after flexural yielding including the deformation capacity of multistory shear walls, is one of the most important factors for the seismic performance of R/C wall-frame structures. In order to analyze shear walls, the hypothesis that plain sections remain plain after bending and that the curvature distribution is proportional to the moment distribution are normally used. However, test results after flexural yielding have indicated that such a hypothesis and method are not applicable. As a result, a truss model consisting of a non-prismatic member and rigid members is proposed in this paper.

There has not been a clear definition as to the deformation capacity yet, which seems to be one of the reasons why the effect of some factors, such as amount of reinforcement, on the deformation capacity has not been clarified. This definition is also examined in detail in this paper.

### DEFORMATION BEHAVIOR OF TEST RESULTS

Deformation Profile The shear walls which represent the lower seven stories of the prototype eleven-story shear walls were tested under reversing static loads in order to investigate the deformation behavior after flexural yielding.<sup>1)</sup> The relationships between the lateral load and the drift angles ( $R_1$  and  $R_4$ ) are shown in Fig. 2, and the deformation profiles along the height of Specimens WF-1 and WF-3 at the imposed drift angle ( $R_1$ ) of 1/200, 1/100, 1/67, 1/50, and 1/30 radians are shown in Fig. 3. Notation used in Figs. 2 and 3 and used hereafter is shown in Fig. 1. Figure 4 gives the ratio of the drift angle  $R_1$  to the drift angle  $R_4$  in order to show clearly the change of the deformation profile according to the

increase in deformation. It is easily found that the deformation profile changed very little after flexural yielding until the drift angle  $R_1$  reached  $1/50$  rad. for both Specimens WF-1 and WF-3. This region is hereafter referred to as the "stable region" of deformation. After the deformation exceeded the limit of this stable region, the deformation profile rapidly changed because a remarkable increase in the deformation of the first story took place and the other stories deformed little except for the horizontal rigid body movement due to the deformation of the first story. Hereafter the region beyond the limit of the stable region is referred to as the "unstable region". These phenomena were caused by either the slippage due to compression in the panel wall or the compression failure at the base of the panel wall and boundary column of the first story.

Figure 5 shows the relationship between the drift angle  $R_1$  and the rotation  $\theta_1$  at the first story. The breaking point of the slope corresponds to the limit of the stable region. Therefore, it is also possible to define the limit of the stable region from the  $R_1$  versus  $\theta_1$  relation.

Rotation at Each Story and at the Hinging Region Figure 6 shows the relationship between the drift angle  $R_1$  and the rotations at the axis of the beam of each story. After flexural yielding of the specimens, the rotation  $\theta_1$  is more than 50% of the rotation  $\theta_4$ , and the rotation  $\theta_2$  is about 90% or more of the rotation  $\theta_4$ . From this fact, it is considered that the hinge formed within the lower two stories. It also found that all the rotations are linearly related to the drift angle  $R_1$  and the rotation above the hinging region has almost the same value as the drift angle  $R_1$  until the deformation reaches the limit of the stable region.

#### TRUSS MODEL EXPRESSING DEFORMATION MECHANISM

Based on the results mentioned above, the truss model shown in Fig. 7, consisting of a non-prismatic member and rigid members, is proposed to express the deformation mechanism in the stable region of shear walls after flexural yielding. This model has been improved from the previous proposal<sup>2)</sup> by considering the length of the hinging region. In this truss model, the cross sectional area of the non-prismatic member is given by Eq. (1) so that the existing stresses of reinforcing bars in the boundary column under tension at a certain height satisfy Eq. (2). Equation (2) is obtained from the equilibrium of forces and moments at an inclined crack surface and at the base (see Fig. 8), where reinforcing bars in the panel wall are assumed to yield at every inclined crack surfaces.

$$A_\eta = \frac{\sigma_o}{\sigma_\eta} A_o \quad (1)$$

$$\sigma_\eta = \frac{T_\eta}{a_t} = \sigma_o - \frac{t p_h \sigma_{wy}}{2 a_t l} \eta^2$$

$$\left\{ \sigma_\eta = 0 \text{ for } \eta \geq \left( (\sigma_o - \sigma_\eta) / \left( \frac{t p_h \sigma_{wy}}{2 a_t l} \right) \right)^{1/2} \right\} \quad (2)$$

where :

$A_\eta, A_o$  = cross sectional areas of the tension chord member, at height  $\eta$  and at the base, respectively,

$\sigma_\eta, \sigma_o$  = existing stresses at the longitudinal reinforcing bars in the boundary column under tension at height  $\eta$  and at the base, respectively,

$a_t$  = sum of the cross sectional area of the longitudinal reinforcing bars in the boundary column under tension,

$t$  = thickness of the panel wall,  $\eta$  = height from the base,

$\sigma_{wy}$  = yield stress of the horizontal reinforcing bars in the panel wall,

$\sigma_y$  = yield stress of the longitudinal reinforcing bars in the boundary column under tension, and

$p_h$  = ratio of the horizontal wall reinforcement.

Figure 9 shows the stresses at the wall reinforcing bars estimated from test results of strains in the two-story shear walls.<sup>3)</sup> The reinforcing bars in the

panel wall did not yield at some points. However, it may be reasonable to consider that the stresses of these reinforcing bars were near the yield stress at the crack surfaces because they are easily affected by the distance between the location of a crack and that of the measurement of the strain.

This truss model deforms by a rigid body rotation due to the stretching of the chord member under tension, where the pivot is located at the base of the boundary column under compression. The strain at a certain height of the tension chord member is determined from Eq. (3) using stress at a certain height defined by Eq. (2), and the stress versus strain relation of steel. The stretching of the tension chord member is calculated by Eq. (4).

$$\epsilon_{\eta} = \epsilon_0 - \frac{t p_h \sigma_{wy}}{2 E_{SH} a_t \ell} \eta^2$$

$$\left\{ \epsilon_{\eta} = 0 \text{ for } \eta \geq \left[ \frac{(\epsilon_0 - \epsilon_{SH})}{\left( \frac{t p_h \sigma_{wy}}{2 E_{SH} a_t \ell} \right)} \right]^{1/2} \right\} \quad (3)$$

$$v_p = \int_0^{\eta} \epsilon_{\eta} d\eta = \frac{1}{3} (2 \epsilon_0 + \epsilon_{SH}) \left[ 2 E_{SH} a_t \ell (\epsilon_0 - \epsilon_{SH}) / (t p_h \sigma_{wy}) \right]^{1/2} \quad (4)$$

where :

$\epsilon_{\eta}$ ,  $\epsilon_0$  = strains at the longitudinal reinforcing bars in the boundary column under tension at height  $\eta$  and the base, respectively,  
 $E_{SH}$  = tangent stiffness module for strain hardening region of steel  
 $\epsilon_{SH}$  = strain at which strain hardening of steel starts, and  
 $v_p$  = stretching of the tension chord member.

The rotation and the drift angle above the hinging region are given by Eq. (5).

$$R_i = \theta_i = R_p = \theta_p = v_p / \ell$$

$$= \frac{1}{3 \ell} (2 \epsilon_0 + \epsilon_{SH}) \left[ 2 E_{SH} a_t \ell (\epsilon_0 - \epsilon_{SH}) / (t p_h \sigma_{wy}) \right]^{1/2} \quad (5)$$

where :

$R_i$ ,  $\theta_i$  = drift angle and rotation of each story above the hinging region, respectively, and  
 $R_p$ ,  $\theta_p$  = drift angle and rotation just above the hinging region.

In Eq. (5), the only unknown factor is  $\epsilon_0$ . Therefore, if  $\epsilon_0$  is obtained by some means,  $R_i$  and  $\theta_i$  are easily calculated, and the effect of factors such as  $a_t / p_h$  on the deformation behavior can be investigated. Figure 10 shows the comparison of analytical and test results of strains in the boundary column under tension for the two-story shear wall.<sup>3)</sup> Figure 11 shows the comparison of analytical and test results of the flexural and shear deformations of Specimens WF-1 and WF-3. The analytical method to distribute the total deformation into shear and flexural deformations are written in References 2, 4 and 5 where the same model of deformation mechanism was used. In Figs. 10 and 11, the analytical results agreed well with the test results.

#### DEFORMATION ABOVE THE HINGING REGION

The truss model shown in Fig. 7 indicates that the drift angle above the hinging region is given by Eq. (6) or by Eq. (7). This drift angle can be also estimated from Eq. (8) assuming that the deformation above the hinging region is caused by the rotation and drift just above the hinging region.

$$R_i = R_p \quad (6) \quad R_i = \theta_p \quad (7)$$

$$R_i = (R_p h_p + \theta_p \times (h_i - h_p)) / h_i \quad (8)$$

where  $h_p$  is the height of the hinging region.

Table 1 gives the ratio of the drift angles above the hinging region estimated by the above three methods to those of the test results. P is taken to be 2 because the hinging region formed within the lower two stories. In the

stable region, any of the methods gives a good estimation of the drift angles above the hinging region. On the other hand, the values estimated from Eqs. (6) and (7) significantly differ from the test results in the unstable region. However, Eq. (8) gives a good estimation of the test results even in this region. The error, 5 to 10%, between the estimated results and the test results in the stable region mainly comes from the fact that the rotation increased a little in the stories above the hinging region (see Fig. 6).

Figure 12 shows the drift angles, of the seventh through eleventh story of the prototype shear walls of the specimens, estimated from Eq. (8) which can estimate deformation even in the unstable region. Here,  $R_1$  and  $\theta_1$  are used as  $R_p$  and  $\theta_p$ . The drift angle  $R_{11}$  of Specimen WF-1 at  $R_1=1/30\text{rad.}$  is less than the drift angle  $R_{11}$  at  $R_1=1/67\text{rad.}$ , and the drift angle  $R_{11}$  of Specimen WF-3 at  $R_1=1/50\text{rad.}$  and  $R_1=1/30\text{rad.}$  increases very little, after  $R_1=1/67\text{rad.}$ , although the hinging region deformed significantly. These facts indicate that the deformation at the limit of the stable region is very important from the viewpoint of overall seismic behavior of multistory shear walls.

On the other hand, it is also found that the deformation may increase further, after the limit of the stable region, without having a remarkable strength reduction when the load versus drift relation at the first story is concerned (see Fig. 2). Therefore, in the studies on deformation capacity of multistory shear walls, it is recommended that the study including test data analysis should be conducted considering the following two deformation capacities:

- (a) The limit of the deformation considering the overall behavior of the multistory shear wall (the deformation at the limit of the stable region), and
- (b) The limit of deformation of the first story, or of a story concerned (the deformation at some notable deterioration in strength, for instance, that at 80% of the maximum strength).

#### CONCLUSIONS

- 1) A stable region of deformation, in which the deformation profile through the height does not change, follows after the flexural yielding of multistory shear walls. In this stable region, shear walls deform in a rotation mechanism having the center of rotation at the base of the boundary column under compression.
- 2) The deformation of the shear walls after flexural yielding can be analytically calculated until the deformation reaches the limit of the stable region only if the strain of the longitudinal bars in the critical section of the boundary column under tension is known. The effect of factors such as amount of reinforcement on the deformation behavior are thus easily investigated.
- 3) In the study of the deformation capacity of multistory shear walls, it is recommended that studies including test data analysis should be conducted at two deformation levels : the deformation at the limit of the stable region and the deformation at which some notable deterioration in strength occurs.
- 4) In the shear wall test, the specimen should be taller than the length of the hinging region expected. The rotation  $\theta_1$ , as well as the drift angle  $R_1$ , should be measured. The stable and the unstable regions should be made distinct based on the  $R_1$  versus  $\theta_1$  relation.

#### ACKNOWLEDGMENTS

The helpful assistance of H. Tomatsuri, PENTA-OCEAN Construction Co., Ltd., is greatly acknowledged for compilation of test data. Also sincere thanks to N. Ishikawa for her editing the manuscript.

REFERENCES

1. Hiraishi, H., Shiohara, H., Kawashima, T., Tomatsuri, H., Kurosawa, A. and Budo, Y., "Experimental Study on Seismic Performance of Multistory Shear Walls with Flanged Cross Section," Ninth World Conference on Earthquake Engineering, Tokyo, (1988).
2. Hiraishi, H., "Evaluation of Shear and Flexural Deformations of Flexural Type Shear Walls," Eight World Conference on Earthquake Engineering, San Francisco, Vol. V, 677-684, (1984).
3. Hiraishi, H. and Kawashima, T., "Experimental Study on Deformation Behavior of Reinforced Concrete Shear Wall After Flexural Yielding (Part-1, Part-2)," Summaries of Technical Papers of Annual Meeting, Architectural Institute of Japan, Kanto, 1941-1944, (1984), (in Japanese).
4. Hiraishi, H., "Analytical Study on Load vs. Deformation Relationship of Flexural Type Reinforced Concrete Shear Walls," Journal of Structural and Construction Engineering (Transactions of AIJ) No. 347, 95-101, Jan., (1985).
5. Hiraishi, H., "An Evaluation Method for Shear and Flexural Deformations of Shear Walls," Transaction of AIJ, 55-62, Nov., (1983), (in Japanese).

Table 1 Ration of Estimated Values ( $R_p = R_z$ ,  $\theta_p = \theta_z$ ) to Test Ones of Drift Angle above Hinging Region

Estimated Method	Stable Region		Unstable Region	
	WF-1	WF-3	WF-1	WF-3
	1/67	1/50	1/30	1/30
3th ~ 6th Story Eq. (6)	1.00~1.05	1.00~1.04	1.24~1.69	1.22~1.33
Eq. (7)	0.86~0.90	0.85~0.88	0.44~0.61	0.74~0.81
Eq. (8)	0.93~0.97	0.92~0.94	0.94~0.97	0.96~0.98

$R_i = R_p$  (6)                       $R_i = \theta_p$  (7)  
 $R_i = (R_p h_p + \theta_p \times (h_i - h_p)) / h_i$  (8)

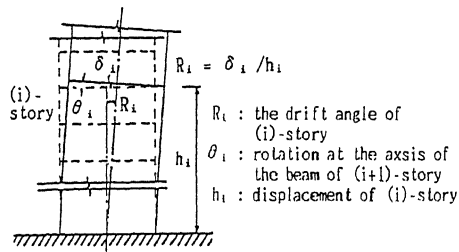


Fig.1 Notation

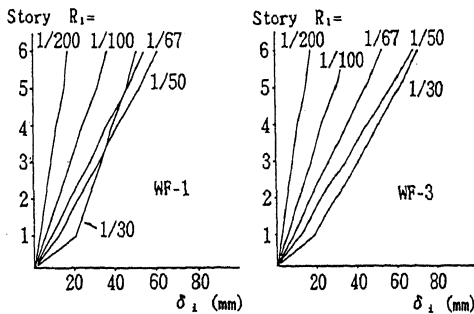


Fig.3 Deformation Profiles along the Height of the Specimens

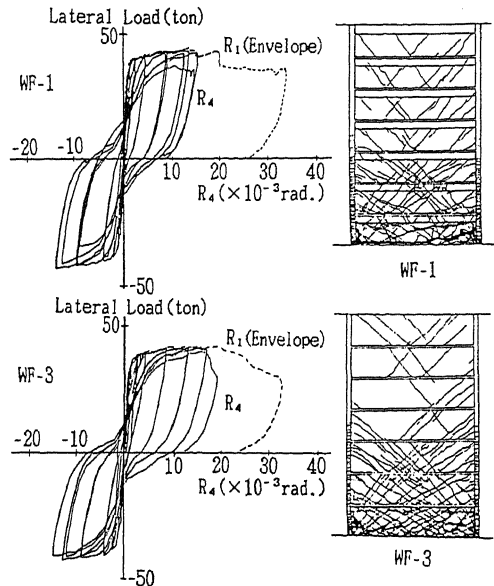


Fig.2 Relationships between the Lateral Load and the Drift Angle and Specimens After Testing

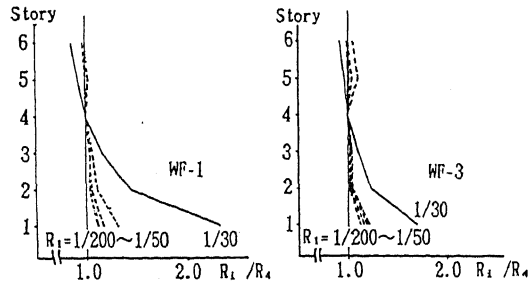


Fig.4 Ratio of Each Drift Angle  $R_i$  to the Drift Angle  $R_a$

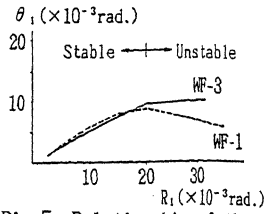


Fig.5 Relationship of the Drift Angle  $R_1$  versus the Rotation  $\theta_1$

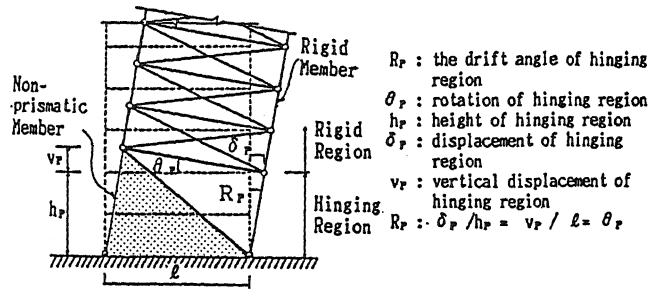


Fig.7 Assumed Truss Model

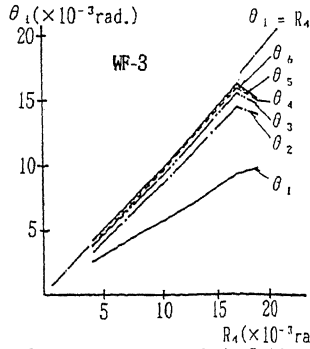


Fig.6 Relationship of the Drift Angle  $R_4$  versus the Rotation Each Story

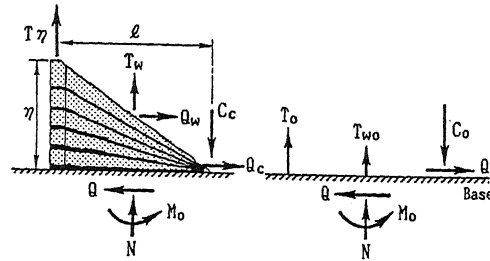


Fig.8 Forces and Moments at a Cracked Surface and the Base

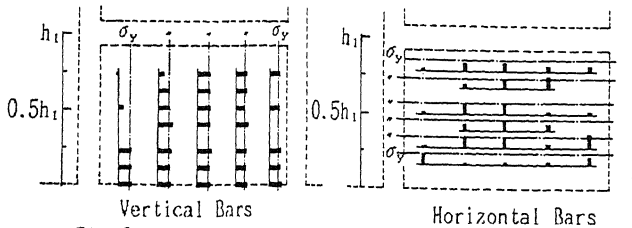


Fig.9 Stresses of Reinforcing Bars in the Panel Wall of Test Results of Strain of Two-story Shear Wall ( $R_1=1/100$ )

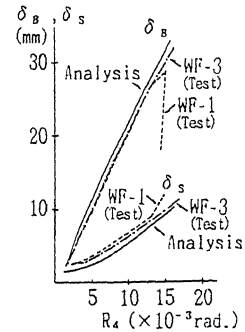


Fig.11 Test and Analytical Results of Flexural and Shear Deformations

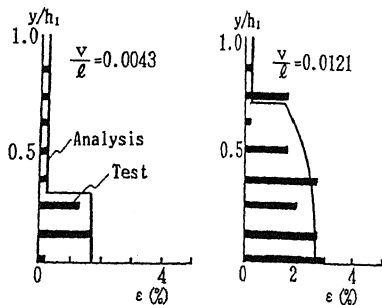


Fig.10 Test and Analytical Results of Strain Distribution along the Height of Main Steel Bars in the Column Under Tension for Two-story Shear Wall<sup>2)</sup>

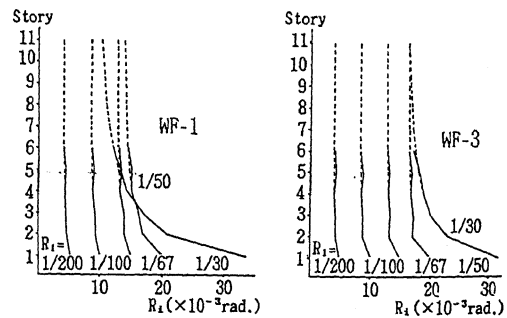


Fig.12 Estimated Drift Angles of Seventh Through Eleventh Stories of the Eleven-story Prototype Shear Walls